Title

Comparing Metastatic Clear Cell Renal Cell Carcinoma Model Established in Mouse Kidney and on Chicken Chorioallantoic Membrane.

Journal

Journal of Visualized Experiments, 2020(156)

ISSN

1940-087X

Authors

Ishihara, Moe
Hu, Junhui
Zhang, Xiaoyu
et al.

Publication Date

2020

DOI

10.3791/60314

Peer reviewed

HHS Public Access

Author manuscript

J Vis Exp. Author manuscript; available in PMC 2021 July 27.

Comparing Metastatic Clear Cell Renal Cell Carcinoma Model Established in Mouse Kidney and on Chicken Chorioallantoic Membrane

Moe Ishihara[*,1], **Junhui Hu**[*,1], **Xiaoyu Zhang**[2], **YongHyeon Choi**[3], **Anthony Wong**[4], **Celine Cano-Ruiz**[5], **Rongwei Zhao**[6], **Ping Tan**[7], **Jonathan L. Tso**[1], **Lily Wu**[1,8]

[1]Department of Molecular and Medical Pharmacology, David Geffen School of Medicine, University of California, Los Angeles, CA, USA

[2]Department of Molecular, Cell, and Developmental Biology, University of California, Los Angeles, CA, USA

[3]Department of Bioengineering, Hanyang University, Seoul, Korea

[4]Department of Ecology and Evolutionary Biology, University of California, Los Angeles, CA, USA

[5]Department of Microbiology, Immunology, and Molecular Genetics, University of California, Los Angeles, CA, USA

[6]School of Life Sciences, Beijing Normal University, Beijing, China

[7]Department of Urology, West China Hospital, Sichuan University, Chengdu, China

[8]Department of Urology, David Geffen School of Medicine, University of California Los Angeles, CA, USA

Abstract

Metastatic clear cell renal cell carcinoma (ccRCC) is the most common subtype of kidney cancer. Localized ccRCC has a favorable surgical outcome. However, one third of ccRCC patients will develop metastases to the lung, which is related to a very poor outcome for patients. Unfortunately, no therapy is available for this deadly stage, because the molecular mechanism of metastasis remains unknown. It has been known for 25 years that the loss of function of the von Hippel-Lindau (VHL) tumor suppressor gene is pathognomonic of ccRCC. However, no clinically relevant transgenic mouse model of ccRCC has been generated. The purpose of this protocol is to introduce and compare two newly established animal models for metastatic ccRCC. The first is renal implantation in the mouse model. In our laboratory, the CRISPR gene editing system was utilized to knock out the VHL gene in several RCC cell lines. Orthotopic implantation of heterogeneous ccRCC populations to the renal capsule created novel ccRCC models that develop robust lung metastases in immunocompetent mice. The second model is the chicken chorioallantoic membrane (CAM) system. In comparison to the mouse model, this model is more

Corresponding Author: Lily Wu (lwu@mednet.ucla.edu).
*These authors contributed equally

DISCLOSURES:
The authors have nothing to disclose.

time, labor, and cost-efficient. This model also supported robust tumor formation and intravasation. Due to the short 10 day period of tumor growth in CAM, no overt metastasis was observed by immunohistochemistry (IHC) in the collected embryo tissues. However, when tumor growth was extended by two weeks in the hatched chicken, micrometastatic ccRCC lesions were observed by IHC in the lungs. These two novel preclinical models will be useful to further study the molecular mechanism behind metastasis, as well as to establish new, patient-derived xenografts (PDXs) toward the development of novel treatments for metastatic ccRCC.

SUMMARY:

Metastatic clear cell renal cell carcinoma is a disease without a comprehensive animal model for thorough preclinical investigation. This protocol illustrates two novel animal models for the disease: the orthotopically implanted mouse model and the chicken chorioallantoic membrane model, both of which demonstrate lung metastasis resembling clinical cases.

Keywords

renal cell carcinoma; metastasis; animal model; renal implantation; CAM; VHL gene deletion; intratumoral heterogeneity

INTRODUCTION:

Renal cell carcinoma (RCC) is the 7th most common cancer in the United States. Annually, 74,000 Americans are estimated to be newly diagnosed, accounting for more than 14,000 deaths (http://seer.cancer.gov/statfacts/html/kidrp.html). Clear-cell histological subtype, or ccRCC, is the most common subtype, accounting for approximately 80% of RCC cases. Patients with localized malignancy are treated with nephrectomy and have a favorable 5-year survival rate of 73%[1]. However, 25%–30% of patients develop distant metastases to vital organs such as the lungs, resulting in a poor mean survival of 13 months and 5-year survival rate of only 11%[1–3]. Further understanding of the metastatic mechanism is needed to improve the deadly outcome for metastatic ccRCC.

The loss of the VHL tumor suppressor gene is a hallmark genetic lesion observed in a majority of human ccRCC cases[4–7]. However, the precise oncogenic mechanism of VHL loss in ccRCC is unknown. Also, VHL expression status is not predictive of outcome in ccRCC[8]. Notably, despite numerous attempts at renal-epithelial-targeted VHL knockout, scientists have failed to generate renal abnormality beyond the preneoplastic cystic lesions observed in mice[9], even when combined with deletion of other tumor suppressors such as PTEN and p53[10]. These findings support the idea that VHL loss alone is insufficient for tumorigenesis or the subsequent spontaneous metastasis.

Recently, our laboratory created a new VHL knockout (VHL-KO) cell line using CRISPR/Cas9 mediated deletion of the VHL gene in the murine VHL+ ccRCC cell line (RENCA, or VHL-WT)[11,12]. We showed that VHL-KO is not only mesenchymal, but also promotes epithelial to mesenchymal transition (EMT) of VHL-WT cells[12]. EMT is known to play an important role in the metastatic process[13]. Our work further showed that distant lung

metastasis occurs only with co-implantation of VHL-KO and VHL-WT cells in the kidney, supporting a cooperative mechanism of metastasis. Importantly, our orthotopically implanted VHL-KO and VHL-WT model leads to robust lung metastases, recapitulating the clinical ccRCC cases. This spontaneous metastatic ccRCC model compensates for the lack of a transgenic metastatic mouse model, especially in the development of novel anti-metastasis drugs. This protocol demonstrates the renal capsule implantation of the heterogeneous cell populations of genetic engineered RENCA cells.

Chicken CAM models have a long history in research for angiogenesis and tumor biology due to their numerous advantages, as summarized in Table 1[14–18]. Briefly, the time window for CAM tumor growth is short, allowing a maximum of 11 days until the CAM is destroyed upon hatching of the chicken[16]. Despite the short growth time, the rich nutrition supply and immunodeficient state of the chicken embryo enable very efficient tumor engraftment[16,19–21]. Finally, the cost of each fertilized egg is ~$1, compared to over $100 for a SCID mouse. Together, the CAM model can serve as a valuable alternative animal model in establishing new PDXs at a great saving in time and cost in comparison to the mouse. In this protocol, we assessed whether the model was able to recapitulate the biology of metastatic ccRCC observed in the mouse orthotopic model.

PROTOCOL:

All methods described here have been approved by the Institutional Animal Care and Use Committee (IACUC), designated as UCLA Chancellor's Animal Research Committee (ARC) (ARC 2002-049-53 and ARC 2017-102-01A). The 2002-049-53 protocol is optimized for the implantation of ccRCC tumor cells into the kidney capsule of Nude or BALB/c mice. Tumor implantation experiments in fertilized chicken eggs prior to hatching does not require IACUC approval. To extend the time for establishment of lung metastasis, the embryos with CAM tumor are allowed to hatch and grow into chickens. The 2017-102-01A protocol covers these animal experiments.

1. Orthotopic tumor studies in mice

NOTE: The timeline for this experiment is shown in Figure 1A. These procedures were adapted from previous publications[11,12].

1.1. Preparing single cell suspension for grafting

1.1.1. Detach the RENCA VHL-WT and VHL-KO cells from the culture dishes using trypsin/EDTA.

1.1.2. Count the cells with a hemocytometer and resuspend in a precooled 1:1 mixture of PBS and extracellular matrix solution at a concentration of 1×10^5 cells/μL.

NOTE: Use a 1:4 ratio of VHL-WT:VHL-KO cells for heterogeneous implants and VHL-WT alone for homogeneous implants.

1.1.3. Transfer the resuspended cells into a 1.5 mL microcentrifuge tube and keep on ice until implantation.

1.2. Implantation to renal capsule

1.2.1. Anesthesia: Preheat a warm pad to 37 °C and cover it with a piece of thick sterile drape. Anesthetize the mouse by either isoflurane inhalation via an induction chamber or intraperitoneal (IP) injection of 1% pentobarbital sodium at the dosage of 10 mL/kg.

1.2.2. Shave the hair from the surgical site. This step can be skipped for nude mice.

1.2.3. Disinfection and surgical draping: Disinfect the back of the mouse entirely with povidone-iodine 3x followed by 70% ethanol 1x and wipe it dry with sterile cotton swabs. Then apply three sterile medical dressings sequentially, covering the whole back in order to create a surgical field as well as to immobilize the mouse.

1.2.4. Incision and kidney exteriorization: Before the operation, disinfect the operator's fingers with povidone-iodine or use a pair of sterile gloves. Place the mouse in the prone position and use the fingers to locate the left kidney right under the left flank. Use a pair of blunt forceps and scissors to cut the skin open and the muscle layer under the specified location. Use sterile cotton swabs and forceps to partially exteriorize the left kidney out of the abdomen.

1.2.5. Tumor cell implantation: Load the cell suspension prepared in step 1.1 in either insulin syringes or customized Hamilton syringes (see Table of Materials for specifications). Inject 20 μL of resuspended cells under the kidney capsule.

NOTE: Successful injection is determined by the formation of a translucent bulge on the surface of the kidney. Accidental injection into the renal parenchyma results in bleeding and a post-operative mortality rate as high as 90% due to fatal hemorrhage at the injection site.

1.2.6. Slowly pull out the needle in order to allow the extracellular matrix solution to solidify and prevent hemorrhage or tumor cell leakage. Then, using a sterile cotton swab, push the kidney back into the abdomen.

1.2.7. Wound stitching: Use a 5–0 coated VICTRYL suture to stitch the muscle layer. Disinfect the skin with povidone-iodine once and close the skin with wound autoclips.

1.2.8. Recovery: Place the mouse on the warm pad until it wakes up. If the mouse was anesthetized by inhalation, withdraw the isoflurane and keep the mouse on the warm pad until it is awake.

1.3. Bioluminescence imaging (BLI) and tissue collection

1.3.1. Six weeks after tumor implantation, take firefly-luciferase-based BLI images. Then euthanize mice with isoflurane inhalation followed by cervical dislocation.

1.3.2. Collect blood for circulating tumor cell (CTC) detection by flow cytometry.

1.3.3. Harvest tumor and organs of interest (kidneys, lungs, liver, intestines, and spleen) using a sterile tissue harvesting technique[22]. Fix them in 4% paraformaldehyde overnight for paraffin-wax embedding.

2. CAM tumor xenograft model

NOTE: These procedures were adapted and modified from previously published protocols[23,24]. The timeline for this procedure is shown in Figure 1B. This article presents only the streamlined protocol. For detailed protocols, please refer to another JoVE article published by our group[25].

2.1. Preincubation: Incubate freshly laid, fertilized chicken eggs in a rotating egg incubator at 37 °C and 55–65% humidity for 7 days.

2.2. Drop the CAM and open window (developmental day 7):

2.2.1. Locate and mark the air sac and veins.

NOTE: Usually 10–15% of the eggs are removed because they are either unfertilized or die within 7 days of fertilization.

2.2.2. Create a new air sac on top of a marked vein.

2.2.3. Delineate the new air sac, apply packing tape, and put the eggs back to the incubator.

NOTE: The procedure can be paused here. It is recommended to resume the procedures within the same day because the air sac may move.

2.2.4. Open a window: Using a pair of curved microdissecting scissors and a pair of needle-nose forceps, cut a 1.5 x 1.5 cm circular window in the shell.

NOTE: Disruption of CAM is indicated by the blood and a piece of CAM present on the cut shell piece.

2.2.5. Seal the hole with transparent medical dressing and place the eggs in a stationary incubator at 37 °C and 55%–65% humidity.

NOTE: Use the same egg incubator as in step 2.1. Turn off the rotator to make it stationary.

2.3. Health check (developmental day 9): Remove dead eggs and then randomly group the rest of the eggs for tumor cell implantation.

NOTE: Ideally, the survival rate at this point is approximately 80% of developmental day 0.

2.4. Grafting the tumor cells onto the newly exposed CAM (developmental day 10)

2.4.1. Dilute the extracellular matrix solution in double the volume of precooled RPMI 1640 (with L-glutamine). Detach the RENCA cells and resuspend in the above solution to reach a concentration of 2×10^4 cells/μL.

NOTE: Use a 1:1 ratio of VHL-WT:VHL-KO cells for heterogeneous implants and VHL-WT alone for homogeneous implantation.

2.4.2. To presolidify the cell suspension, fill 100 μL of each cell mix in 200 μL pipette tips and place them in a cell incubator for 15 mins.

2.4.3. Implant 100 μL of cell suspension for each egg on the CAM surface through the window.

NOTE: Some protocols require scratching the CAM before implantation[23]. This is not necessary for RENCA cells, because they grow very quickly.

2.5. Grow cells on the CAM for 10 days and photograph every 2 days.

2.6. Euthanize and harvest the tumor, blood, and organs.

2.6.1. On developmental day 20 (tumor day 10), collect blood via the chorioallantoic vein with a heparinized 10 mL syringe.

2.6.2. Euthanize the embryos by putting them on ice for 15 min.

2.6.3. Harvest and weigh tumors. Dissect lungs and livers using a sterile tissue harvesting technique similar to that used for mice[22].

NOTE: Chickens livers have two lobes, which are the first organs seen in the abdominal cavity. Do not confuse these with the lungs. The chicken lungs are located under the heart and septum[26]. The successful collection of the lungs can be confirmed by exposed ribs.

2.6.4. Fix the tumors and the dissected organs in 4% paraformaldehyde overnight for paraffin-wax embedding.

2.7. Hatch the chickens.

2.7.1. To allow an extended period of tumor growth, continue the incubation through day 21 and let the chickens hatch at 37 °C and at least 60% humidity.

NOTE: Chickens naturally hatch after day 21 over a 24 h time period but occasionally have trouble hatching by themselves. In this

case, cracking the eggshells some helps. It is important for chickens to complete the hatching process within 24 h because they will die from lack of nutrients after then.

2.7.2. Grow the chickens in an animal facility (2017-102-01A) for 2 weeks.

2.7.3. On developmental day 34 (tumor day 24), euthanize the chicks with isoflurane inhalation followed by cervical dislocation.

2.7.4. Dissect the lungs using a sterile tissue harvesting technique similar to those used for mice[22]. Then, fix them in 4% paraformaldehyde overnight for paraffin-wax embedding.

3. Immunohistochemistry

NOTE: All tissue sectioning and H&E staining was done by the Translational Pathology Core Laboratory (TPCL) at the University of California, Los Angeles.

3.1. Bake slides at 65 °C for 20 min and deparaffinize 3x using xylene and rehydrate serially from 100% ethanol to water.

3.2. Retrieve the antigens in a citrate buffer boiled in a vegetable steamer for 25 min.

3.3. Apply 1% BSA for blocking. Then apply the primary antibodies (anti-VHL, anti-HA, anti-flag) prepared at a 1:200 dilution ratio in PBS. Incubate overnight at 4 °C.

3.4. After washing 3x with TBST (7 min each), incubate slides with the secondary antibody at 1:200 dilution. Wash 3x with TBST (7 min each) and apply DAB reagents followed by hematoxylin counterstaining.

4. Flow Cytometry

4.1. Process the mouse or chicken blood with red blood cell (RBC) lysis buffer according to the manufacturer's protocol.

NOTE: Sufficient RBC lysis is especially important when analyzing CAM blood because chicken RBCs are nucleated and cannot be easily distinguished in flow cytometry using the forward and side scatter.

4.2. Run flow cytometry on the blood lysate and analyze the data for mStrawberry and EGFP expression.

4.3. Set the primary gates based on the forward and side scatter excluding debris, dead cells, and unlysed RBCs.

4.4. Set the fluorescence gates based on the unstained samples and single stained controls. Use blood lysate primed with VHL-WT, VHL-KO, or unlabeled RENCA cells as the single stained controls and unstained controls, respectively.

REPRESENTATIVE RESULTS:

Each experiment was performed at least 3x unless otherwise stated. Data are presented as mean ± standard deviation (SD). Significance was determined by a paired, Student's T-test when there were two groups or by a one-way ANOVA when there were three or more groups. A p-value cutoff of 0.05 was used to establish significance.

Orthotopically implanted RENCA cells successfully grew on the mice kidneys, as confirmed by BLI and H&E staining (Figure 2A–B). Although there was no difference in the primary growth, only the heterogeneous, metastatic tumor had robust metastasis to the lung as indicated by the very strong BLI signal and metastatic nodules in the H&E staining. On the other hand, homogeneous, nonmetastatic tumors did not metastasize to distant organs. CTC counts were higher in the mice bearing metastatic tumors than those bearing nonmetastatic tumors (Figure 2C, D).

In concordance with the mouse model, the CAM system successfully retained the growth and metastatic behavior of the RENCA tumors. While there was no growth difference between metastatic and nonmetastatic tumors, the CTC counts were significantly higher in the eggs with metastatic tumors than those with nonmetastatic counterparts (Figure 3A–C). Hatching the eggs with CAM tumors and allowing the chicks to grow an additional two weeks extended the period for metastatic cancer cells to establish histologically detectable metastases in the lung of chicks, as shown in the H&E and HA stain of chicken lung tissue sections (Figure 3D). A majority of the metastatic nodules consisted of HA-tagged VHL-WT cells, whereas flag-tagged VHL-KO were rarely seen, as we have observed in mice.

DISCUSSION:

For many patients with epithelial malignancies, metastasis to vital organs is the primary cause of mortality. Therefore, it is essential to find the underlying mechanism and a new avenue of therapy for metastatic disease. Unfortunately, there is a lack of relevant metastatic ccRCC animal models. The challenge in large part is due to the inability to recreate ccRCC in mice despite the generation of numerous transgenic kidney epithelial-targeted VHL knockout mouse models[9,10]. Here, we demonstrate the methods to establish an implantable metastatic ccRCC tumor in two animal systems, the mouse and the chicken CAM. These findings validated the metastatic behavior of the tumors in two disparate environments, and thus provide unique opportunities to further investigate the molecular mechanism of metastasis. In the first model, the heterogeneous RENCA population was implanted to immunocompetent mice orthotopically to their renal capsule. After 6 weeks, these mice showed rampant lung metastasis. In concordance with the mouse model, implantation of heterogeneous RENCA cells on the CAM successfully grew and intravasated into the blood of the chick embryos. By extending the tumor growth period to 2 weeks after hatching, lung metastases resembling those seen in the mouse were observed in the chicks.

For both models, careful attention to the technical details of each step and practice to improve technical skills are essential to increase animal survival and successful tumor engraftment and metastasis. For the mouse model, careful choice of equipment and accurate

injection of the tumor cells to the renal capsule maximizes the success rate by decreasing the post-operative mortality and increasing the chance for the tumor to get an adequate blood supply to grow and metastasize. The CAM model requires more optimization in the setup and the technique. In our studies, the embryo viability was below 30% at the beginning. It is important to keep both the temperature and humidity to the desired level at all times by having good equipment, frequent monitoring, and faster completion of the procedures. Even after optimization, the survivability ranges from 50–75% depending on the experimenter and the individual batch of eggs. It is recommended to always order extra eggs for backup. In our experience, mastering the CAM techniques requires over 1 year. Dropping the CAM membrane and opening the window is the critical step where accidental, fatal damage to the embryo most often occurs. The viability of the chick embryo can be improved by preventing damage to the CAM.

There are several limitations to the CAM tumor model. First is the applicability of the model to all tumor cell types. We have had a 100% success rate engrafting different established tumor cell lines on CAM, including kidney, bladder, and prostate tumor cell lines (RENCA, ACHN, T24, HT1376, CWR22Rv1, C4–2, Myc-CaP) and ovarian cancer cell lines (ID8 and SKOV3). Two additional studies from our group provide further information on these CAM tumors[25,27]. However, the growth of some ovarian cancer cells on CAM is enhanced by the supplementation of growth factor or tumor-associated cells[25]. The optimization of cell number or essential growth factor(s) for each cell line or type is important. We also incorporate reporter or marker genes, such as luciferase, protein tags (e.g., HA or flag), or fluorescence tags (e.g., mStrawberry or EGFP), to facilitate the monitoring of the growth and metastasis of the tumor in the animals[25,27]. Based on our experience, a large majority of proliferating cancer cell lines can be established on CAM. A key limitation to engraftment might be the short 10 day window allowed for tumor growth, which could be especially challenging for a slow growing cell line to establish sufficient mass in such a short time frame.

Another shortcoming of the CAM model is the difference in physiology between the avian embryo and mammals. Metastasis from the CAM tumor to major organs such as the liver or lungs of the embryo has been detected predominantly by sensitive PCR techniques[28]. The short time period of growth in CAM would be insufficient to establish large metastatic lesions that can be verified by histological analyses. Furthermore, the reduced vascular perfusion of the uninflated embryo lung is not favorable for establishing or supporting the growth of lung metastases. To overcome these limitations, an approval from our institutional animal use committee (IACUC) was obtained to hatch chickens from the CAM tumor bearing embryos and house them an additional 2 weeks after hatching. Extending the time of tumor growth in this manner enabled us to detect distant lung metastases by IHC. Although the hatched chicken studies require the additional IACUC approval that CAM tumor studies do not, this approach provides a valuable opportunity to study the metastatic cascade in chickens as previously done in mice. The chicken immune system has been reported to develop starting on day 12 post fertilization[20]. Given the high efficiency of engrafting murine derived RENCA tumors reported here and many other human cancer cell lines and PDXs in the CAM on day 10 after fertilization[24,25,27], we could deduce that the immune

system in the embryo is not fully developed at this point. The interplay of the chicken's immune system and the CAM tumor clearly warrants further investigation.

Our work provides strong supportive evidence that the CAM tumor model could be a simple initial in vivo model to study cancer biology, including metastasis. Due to the limitations noted above, the CAM model should not replace the mouse model, but complement it. Our ongoing research suggests that signal crosstalk between heterogeneous cell populations in ccRCC is instrumental in governing metastatic progression[11,12]. The use of both the CAM and mouse models can be a valuable means to validate the metastatic crosstalk at play in ccRCC. We believe the numerous advantages of the CAM model presented here could accelerate the pace of discovery of novel metastatic mechanisms and effective treatments to remedy this deadly stage of cancer.

Supplementary Material

Refer to Web version on PubMed Central for supplementary material.

ACKNOWLEDGMENTS:

This work was funded by the UCLA JCCC seed grant, UCLA 3R grant, UCLA CTSI, and UC TRDRP (LW). We thank the Crump Institute's Preclinical Imaging Facility, the TPCL, and UCLA's Department of Laboratory Animal Medicine (DLAM) for their help with experimental methods. Flow cytometry was performed in the UCLA Johnson Comprehensive Cancer Center (JCCC) and Center for AIDS Research Flow Cytometry Core Facility that is supported by National Institutes of Health awards P30 CA016042 and 5P30 AI028697, and by the JCCC, the UCLA AIDS Institute, the David Geffen School of Medicine at UCLA, the UCLA Chancellor's Office, and the UCLA Vice Chancellor's Office of Research. Statistics consulting and data analysis services were provided by the UCLA CTSI Biostatistics, Epidemiology, and Research Design (BERD) Program that is supported by NIH/National Center for Advancing Translational Science UCLA CTSI Grant Number UL1TR001881.

REFERENCES:

1. Cohen HT, McGovern FJ Renal-cell carcinoma. The New England Journal of Medicine. 353 (23), 2477–2490 (2005). [PubMed: 16339096]
2. Bianchi M et al. Distribution of metastatic sites in renal cell carcinoma: a population-based analysis. Annals of Oncology. 23 (4), 973–980 (2012). [PubMed: 21890909]
3. Hsieh JJ et al. Renal cell carcinoma. Nature Reviews Disease Primers. 3, 17009 (2017).
4. Foster K et al. Somatic mutations of the von Hippel-Lindau disease tumour suppressor gene in non-familial clear cell renal carcinoma. Human Molecular Genetics. 3 (1994).
5. Young AC et al. Analysis of VHL Gene Alterations and their Relationship to Clinical Parameters in Sporadic Conventional Renal Cell Carcinoma. Clinical Cancer Research. 15 (24), 7582–7592 (2009). [PubMed: 19996202]
6. Gossage L, Eisen T, Maher ER VHL, the story of a tumour suppressor gene. Nature Reviews Cancer. 15 (1), 55–64 (2015). [PubMed: 25533676]
7. Sato Y et al. Integrated molecular analysis of clear-cell renal cell carcinoma. Nature Genetics. 45 (8), 860–867 (2013). [PubMed: 23797736]
8. Choueiri TK et al. The role of aberrant VHL/HIF pathway elements in predicting clinical outcome to pazopanib therapy in patients with metastatic clear-cell renal cell carcinoma. Clinical Cancer Research. 19 (18), 5218–5226 (2013). [PubMed: 23881929]
9. Hsu T Complex cellular functions of the von Hippel-Lindau tumor suppressor gene: insights from model organisms. Oncogene. 31 (18), 2247–2257 (2012). [PubMed: 21996733]
10. Albers J et al. Combined mutation of Vhl and Trp53 causes renal cysts and tumours in mice. EMBO Molecular Medicine. 5 (6), 949–964 (2013). [PubMed: 23606570]

11. Schokrpur S et al. CRISPR-Mediated VHL Knockout Generates an Improved Model for Metastatic Renal Cell Carcinoma. Scientific Reports. 6, 29032 (2016). [PubMed: 27358011]
12. Hu J et al. A Non-integrating Lentiviral Approach Overcomes Cas9-Induced Immune Rejection to Establish an Immunocompetent Metastatic Renal Cancer Model. Molecular Therapy Methods & Clinical Development. 9, 203–210 (2018). [PubMed: 29766028]
13. Heerboth S et al. EMT and tumor metastasis. Clinical and Translational Medicine. 4, 6 (2015). [PubMed: 25852822]
14. DeBord LC et al. The chick chorioallantoic membrane (CAM) as a versatile patient-derived xenograft (PDX) platform for precision medicine and preclinical research. American Journal of Cancer Research. 8 (8), 1642–1660 (2018). [PubMed: 30210932]
15. Hagedorn M et al. Accessing key steps of human tumor progression in vivo by using an avian embryo model. Proceedings of the National Academy of Sciences of the United States of America. 102 (5), 1643–1648 (2005). [PubMed: 15665100]
16. Ribatti D The chick embryo chorioallantoic membrane as a model for tumor biology. Experimental Cell Research. 328 (2), 314–324 (2014). [PubMed: 24972385]
17. Ismail MS et al. Photodynamic Therapy of Malignant Ovarian Tumours Cultivated on CAM. Lasers in Medical Science. 14 (2), 91–96 (1999). [PubMed: 24519162]
18. Kaufman N, Kinney TD, Mason EJ, Prieto LC Jr. Maintenance of human neoplasm on the chick chorioallantoic membrane. The American Journal of Pathology. 32 (2), 271–285 (1956). [PubMed: 13302398]
19. Janse EM, Jeurissen SH Ontogeny and function of two non-lymphoid cell populations in the chicken embryo. Immunobiology. 182 (5), 472–481 (1991). [PubMed: 1916887]
20. Leene W, Duyzings MJ, van Steeg C Lymphoid stem cell identification in the developing thymus and bursa of Fabricius of the chick. Zeitschrift fur Zellforschung und Mikroskopische Anatomie. 136 (4), 521–533 (1973). [PubMed: 4734410]
21. Solomon JB in Foetal and neonatal immunology Frontiers of biology, xv, 381 p. with illus. (North-Holland Pub. Co., 1971).
22. JoVE Science Education Database. Lab Animal Research. Sterile Tissue Harvest. JoVE, Cambridge, MA. (2019).
23. Palmer TD, Lewis J, Zijlstra A Quantitative analysis of cancer metastasis using an avian embryo model. Journal of Visualized Experiments. (51), e2815 (2011).
24. Fergelot P et al. The experimental renal cell carcinoma model in the chick embryo. Angiogenesis. 16 (1), 181–194 (2013). [PubMed: 23076651]
25. Sharrow AC, Ishihara M, Hu J, Kim IH, Wu L Using the Chicken Chorioallantoic Membrane In Vivo Model to Study Gynecological and Urological Cancers. JoVE. (In Press).
26. Lőw P, Molnár K, Kriska G in Atlas of Animal Anatomy and Histology. pp. 265–324 (2016).
27. Hu J, Ishihara M, Chin AI, Wu L Establishment of xenografts of urological cancers on chicken chorioallantoic membrane (CAM) to study metastasis. Precision Clinical Medicine. 2 (3), 140–151 (2019). [PubMed: 31598385]
28. Casar B et al. In vivo cleaved CDCP1 promotes early tumor dissemination via complexing with activated beta1 integrin and induction of FAK/PI3K/Akt motility signaling. Oncogene. 33 (2), 255–268 (2014). [PubMed: 23208492]

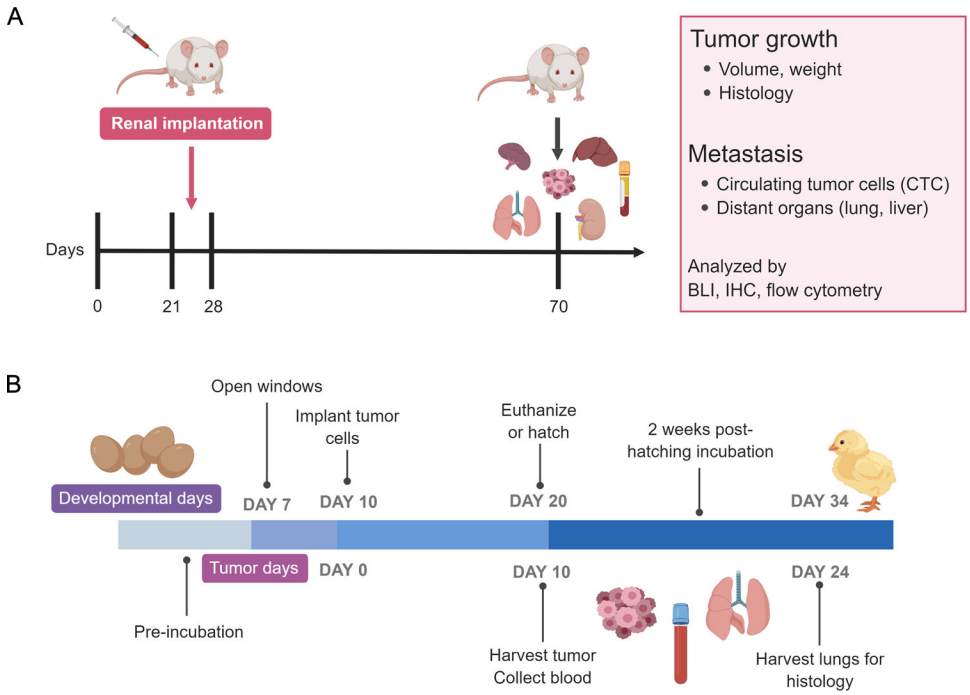

Figure 1: Overview of the two animal models for metastatic ccRCC xenografts.

(**A**) Schematic representation of the mouse orthotopic model. 3- or 4-week-old mice are orthotopically implanted with either nonmetastatic or metastatic tumors. Six weeks after implantation, tumor growth and metastasis were visualized with BLI. Then, tumor, blood, and organs were collected for downstream analyses. (**B**) Schematic representation of the CAM model showing the following steps: Preincubation, window opening, cell implantation, and euthanasia before or after hatching. The same analyses as the mouse model are conducted for the collected samples.

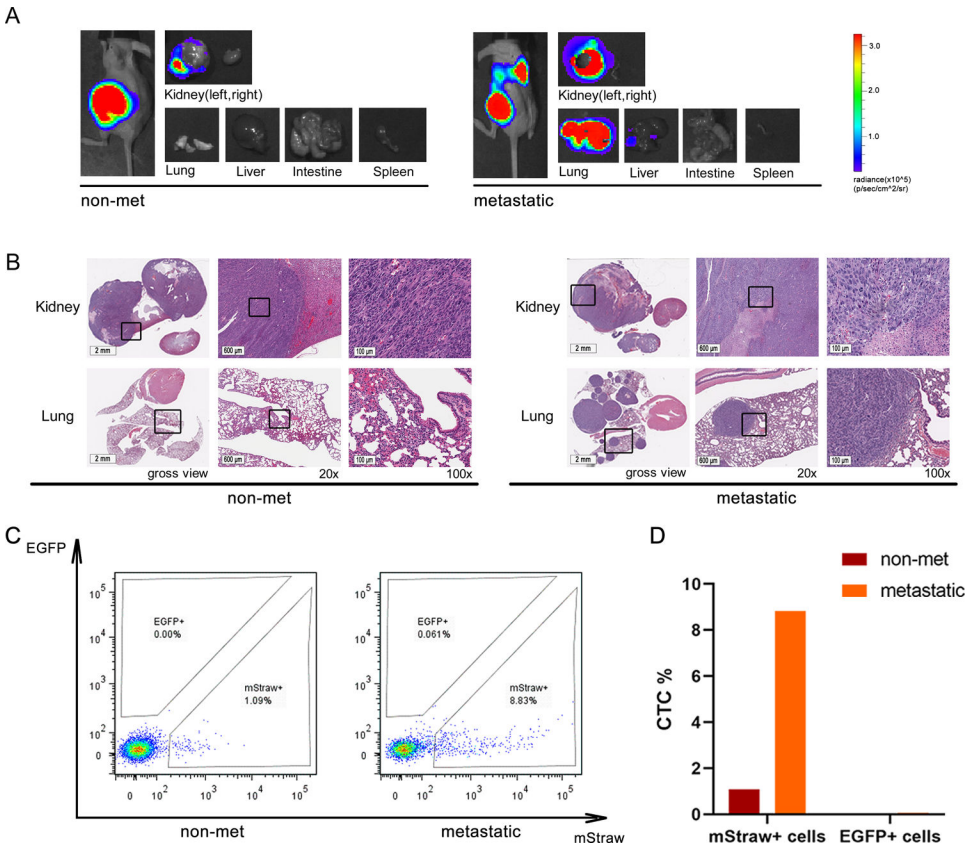

Figure 2: Tumor growth and metastasis in orthotopically implanted mice.

(**A**) BLI of mice and extracted organs (kidney, lung, liver, intestine, and spleen) 6 weeks after orthotopic implantation of RENCA cells. Left: nonmetastatic (non-met), right: metastatic. (**B**) Gross view and increasing magnification of H&E staining for the kidney and lung (20x and 100x). Left: nonmetastatic (non-met), right: metastatic. (**C**) Representative flow analysis for detecting mStraw+ and EGFP+ cells circulating in the blood. (**D**) Percent population graph of circulating mStraw+ and EGFP+ cells. Non-met: nonmetastatic. Panel A was adapted from Hu et al.[27].

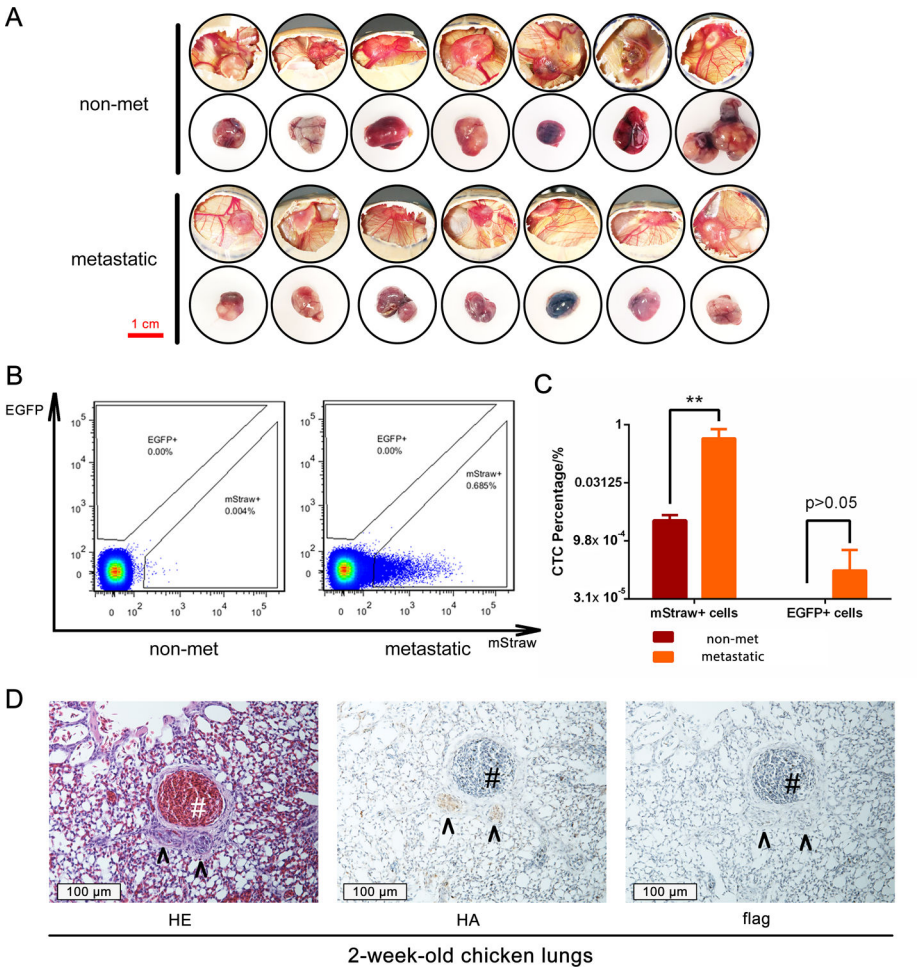

Figure 3: Tumor growth and metastasis in the CAM model.

(**A**) RENCA tumors grown in CAM. There were 7 repeats for each group. Non-met: nonmetastatic. (**B**) Representative flow analysis for detecting mStraw+ and EGFP+ cells circulating in the blood. (**C**) Percent population graph of circulating mStraw+ and EGFP+ cells. **p < 0.01. (**D**) IHC staining of the lung from a 2-week-old chick bearing a metastatic tumor during its embryonic stage. From left, the sections show H&E, HA, and flag staining. #: chicken pulmonary artery; arrowhead: metastatic nodules. This figure was adapted from Hu J et al.[27].

Table 1:
Advantages and limitations of the mouse and CAM models.

This table compares the two models for their advantages and limitations in terms of required time, cost, labor, as well as the biology. The CAM model has advantages in efficiency, but it also has its own unique limitations due to the different morphology between birds and mammals. Therefore, it is important to confirm that the model can retain the biology of the xenografts.

	(SCID) Mouse	CAM	Note
Cost	>$100 each	~$1 each	Viability ranging from 50–75%
Need for barrier housing	Yes	No	Further reduces cost & simplifies serial monitoring of the tumors
Tumor directly visible	No	Yes	Figure 3A
Time to first engraftment (RENCA)	2 weeks	2–4 days	ref 14, 15
Endpoint of growth (RENCA)	3–6 weeks	10 days	ref 14, 15
Metastasis (RENCA) observed	Yes	Yes in chicks	Figure 3D
Serial passages	Yes	Yes	ref 16–18
Passage to mice (RENCA)	Yes	Yes	Hu, J., et al. under review (2019)
Maintain tumor heterogeneity	Yes	Yes	Hu, J., et al. under review (2019)

Table of Materials.

Name of Material/ Equipment	Company	Catalog Number	Comments
Cell Culture			
RPMI 1640 Medium (Mod.) 1X with L-Glutamine	Corning	10040CV	
Fetal Bovine Serum, Qualified, USDA-approved Regions	Fisher Scientific	10-437-028	
Penicillin-Streptomycin Sollution, 100X, 10,000 IU Penicillin, 10,000ug/mL Streptomycin	Fisher Scientific	MT-30-002-CI	
Puromycin dihydrochloride hydrate, 99%, ACROS Organics	Fisher Scientific	AC227420500	
Scientific 96-Well Non-Skirted Plates, Low Profile	Fisher Scientific	AB-0700	
pSicoR	Addgene	11579	
Renca	ATCC	CRL-2947	
VHL-WT			Lentivirally labeled with HA-tagged mStrawberry fluorescent protein & firefly luciferase
VHL-KO			CRISPR/Cas9-mediated knockout of VHL, then lentivirally labeled with flag-tagged EGFP & firefly luciferase
0.25% Trypsin, 0.1% EDTA in HBSS w/o Calcium, Magnesium and Sodium Bicarbonate	Corning	25053CI	
DPBS without Calcium and Magnesium	Gibco	LS14190250	
Matrigel GFR Membrane Matrix	Corning	C354230	
Hemocytometer	Hausser Scientific	3100	
Fisherbrand Premium Microcentrifuge Tubes: 1.5mL	Fisher Scientific	05-408-129	
Orthotopic implantation			
Medline Surgical Instrument Drape, Clear Adhesive, 24” x 18”	Medex Supply	MED-DYNJSD2158	
Pentobarbital Sodium	Sigma Aldrich	57-33-0	Prepare 1% in saline
Povidone-Iodine Solution USP, 10% (w/v), 1% (w/v) Available Iodine, for Laboratory Use	Ricca Chemical	395516	
Ethanol 200 Proof	Cylinders Management	43196-11	Prepare 70% in water
Fisherbrand Sterile Cotton Balls	Fisher Scientific	22-456-885	
Tegaderm Transparent Dressing Original Frame Style 2 3/8” x 2 3/4”	Moore Medical	1634	
World Precision Instrument FORCEPS IRIS 10CM CVD SERR	Fisher Scientific	50-822-331	
Fisherbrand Sharp-Pointed Dissecting Scissors	Fisher Scientific	08-940	
BD Lo-Dose U-100 Insulin Syringes	BD Biosciences	14-826-79	
Hamilton customized syringe	Hamilton	80408	25 μL, Model 702 SN, Gauge: 30, Point Style: 4, Angle: 30, Needle Length: 17mm
Suture	Ethicon	J385H	

Name of Material/ Equipment	Company	Catalog Number	Comments
Wound autoclips kit	Braintree scientific, inc.	ACS KIT	
Isothesia (Isoflurane) solution	Henry Schein Animal Health	1169567762	
Formaldehyde Soln., 4%, Buffered, pH 6.9 (approx. 10% Formalin soln.), For Histology	MilliporeSigma	1.00496.5000	
CAM			
Hovabator Genesis 1588 Deluxe Egg Incubator Combo Kit	Incubator Warehouse	HB1588D	
8050-N/18 Micro 8V Max Tool Kit	Dremel	8050-N/18	
BD General Use and PrecisionGlide Hypodermic Needles	Fisher Scientific	14-826-5D	
Tygon Clear Laboratory Tubing - 1/4 × 3/8 × 1/16 wall (50 feet)	Tygon	AACUN017	
Shipping Tape, Multipurpose, 1.89” × 109.4 Yd., Tan, Pack Of 6 Rolls	Office Depot	220717	
Thermo-Chicken Heated Pad	K&H manufacturing	1000	
Fisherbrand High Precision Straight Tapered Ultra Fine Point Tweezers/Forceps	Fisher Scientific	12-000-122	
SHARP Precision Barrier Tips, For P-200, 200µl, 960 (10 racks of 96)	Thomas Scientific	1159M40	
Immunohistochemistry			
Xylenes (Histological), Fisher Chemical	Fisher Scientific	X3S-4	
OmniPur BSA, Fraction V [Bovine Serum Albumin] Heat Shock Isolation	MilliporeSigma	2910-25GM	
anti-VHL antibody	Abcam	ab135576	
HA-probe Antibody (Y-11)	Santa Cruz Biotechnology	sc805	
DYKDDDDK Tag Monoclonal Antibody (FG4R)	eBioscience	14-6681-82	
Peroxidase AffiniPure Goat Anti-Rabbit IgG (H+L)	Jackson ImmunoResearch Laboratories	111-035-045	
Peroxidase AffiniPure Goat Anti-Mouse IgG (H+L)	Jackson ImmunoResearch Laboratories	115-035-062	
DAB Chromogen Kit	Biocare Medical	DB801R	
Flow cytometry			
BD Pharm Lyse	BD Biosciences	555899	
Bioluminescence imaging			
D-Luciferin Firefly, potassium salt	Goldbio	LUCK-1G	
IVIS Lumina II In Vivo Imaging System	Perkin Elmer		